*Physiol Genomics* 56: 634–647, 2024.
*First published July 22, 2024; doi:10.1152/physiolgenomics.00119.2023*

american physiological society | PHYSIOLOGICAL GENOMICS

RESEARCH ARTICLE

# Genetic drivers of age-related changes in urinary magnesium excretion

**Wouter H. van Megen,[1] Jeroen H. F. de Baaij,[1] Gary A. Churchill,[2] Olivier Devuyst,[3] Joost G. J. Hoenderop,[1] and Ron Korstanje[2]**

[1]*Department of Medical Biosciences, Radboudumc, Nijmegen, The Netherlands;* [2]*The Jackson Laboratory, Bar Harbor, Maine, United States; and* [3]*Institute of Physiology, University of Zurich, Zurich, Switzerland*

## Abstract

Although age-dependent alterations in urinary magnesium ($Mg^{2+}$) excretion have been described, the underlying mechanism remains elusive. As heritability significantly contributes to variations in urinary $Mg^{2+}$ excretion, we measured urinary $Mg^{2+}$ excretion at different ages in a cohort of genetically variable Diversity Outbred (DO) mice. Compared with animals aged 6 mo, an increase in $Mg^{2+}$ excretion was observed at 12 and 18 mo. Quantitative trait locus (QTL) analysis revealed an association of a locus on chromosome 10 with $Mg^{2+}$ excretion at 6 mo of age, with *Oit3* (encoding oncoprotein-induced transcript 3; OIT3) as our primary candidate gene. To study the possible role of OIT3 in renal $Mg^{2+}$ handling, we generated and characterized *Oit3* knockout (*Oit3*$^{-/-}$) mice. Although a slightly lower serum $Mg^{2+}$ concentration was present in male *Oit3*$^{-/-}$ mice, this effect was not observed in female *Oit3*$^{-/-}$ mice. In addition, urinary $Mg^{2+}$ excretion and the expression of renal magnesiotropic genes were unaltered in *Oit3*$^{-/-}$ mice. For animals aged 12 and 18 mo, QTL analysis revealed an association with a locus on chromosome 19, which contains the gene encoding TRPM6, a known $Mg^{2+}$ channel involved in renal $Mg^{2+}$ reabsorption. Comparison with RNA sequencing (RNA-Seq) data revealed that *Trpm6* mRNA expression is inversely correlated with the QTL effect, implying that TRPM6 may be involved in age-dependent changes in urinary $Mg^{2+}$ excretion in mice. In conclusion, we show here that variants in *Oit3* and *Trpm6* are associated with urinary $Mg^{2+}$ excretion at distinct periods of life, although OIT3 is unlikely to affect renal $Mg^{2+}$ handling.

**NEW & NOTEWORTHY** Aging increased urinary magnesium ($Mg^{2+}$) excretion in mice. We show here that variation in *Oit3*, a candidate gene for the locus associated with $Mg^{2+}$ excretion in young mice, is unlikely to be involved as knockout of *Oit3* did not affect $Mg^{2+}$ excretion. Differences in the expression of the renal $Mg^{2+}$ channel TRPM6 may contribute to the variation in urinary $Mg^{2+}$ excretion in older mice.

*genetic analysis; magnesium; mouse; OIT3; TRPM6*

## INTRODUCTION

Magnesium ($Mg^{2+}$) is a crucial cofactor for many enzymatic processes and hence influences numerous physiological processes, including muscle contractility, immune system function, and neurotransmission (1). The serum $Mg^{2+}$ level is kept within a narrow range of 0.7–1.1 mmol/L through the interplay between intestinal uptake, storage in bone, and excretion by the kidneys (1). Importantly, although the serum $Mg^{2+}$ level generally does not change upon aging, several studies do imply alterations in $Mg^{2+}$ homeostasis in the elderly (2–5). Indeed, inadequate dietary $Mg^{2+}$ consumption, reduced intestinal $Mg^{2+}$ absorption, and increased urinary $Mg^{2+}$ excretion have been proposed (2, 6). In addition, elderly people might be more susceptible to hypomagnesemia following treatment with the thiazide class of diuretics (7). Experiments using rats showed decreased urinary $Mg^{2+}$ excretion upon aging, whereas clinical data from elderly subjects also indicates increased renal $Mg^{2+}$ retention (4, 8). In addition to these alterations in $Mg^{2+}$ homeostasis in elderly subjects, alterations in serum and urinary $Mg^{2+}$ levels have also been found in children: the serum $Mg^{2+}$ concentration is inversely corrected with age in children, whereas the fractional urinary excretion of $Mg^{2+}$ is positively correlated with age in children (9). However, the mechanisms underlying alterations in urinary $Mg^{2+}$ excretion at different ages are currently unclear. Nevertheless, in aging rats, the urinary excretion of orally administered copper and zinc was not significantly different compared with younger rats, whereas urinary $Ca^{2+}$ excretion increased with age (8). Furthermore, in elderly people, no delay in urinary $Mg^{2+}$ excretion was observed after an oral $Mg^{2+}$ load compared with controls (4). This suggests that the lower urinary $Mg^{2+}$ excretion upon aging does not reflect a decline in kidney function.

Previous research has revealed the existence of a strong genetic contribution to variations in serum and urinary $Mg^{2+}$ levels (10–12). For serum $Mg^{2+}$, twin studies and family-based cohorts originating from the general population suggested a heritability of 27%–32% (10, 12). Heritability for urinary $Mg^{2+}$ was reported to be around 28% for urinary

Correspondence: R. Korstanje (ron.korstanje@jax.org).
Submitted 13 October 2023 / Revised 1 July 2024 / Accepted 2 July 2024

clearance and fractional excretion and 29%–34% for total urinary excretion (11, 12). Previous genome-wide association studies (GWAS) have linked single-nucleotide polymorphisms (SNPs) in *TRPM6*, which encodes a $Mg^{2+}$ channel in the colon and kidney that facilitates $Mg^{2+}$ (re)absorption, to variations in serum $Mg^{2+}$ and urinary $Mg^{2+}$ excretion (13–16). Moreover, one of these studies also linked *ARL15* to renal $Mg^{2+}$ handling, illustrating the capability of GWAS to discover novel genes associated with a phenotype. However, *TRPM6* and *ARL15* variants explained only 2.3% of the variation in urinary $Mg^{2+}$ excretion, suggesting that currently undiscovered genetic variants also contribute to the genetic component of urinary $Mg^{2+}$ excretion (13).

To better understand the mechanism underlying changes in urinary $Mg^{2+}$ excretion with age, we used a large cohort of Diversity Outbred (DO) mice, which were derived from eight founder inbred strains (17). In contrast to commonly used inbred mice, the high genetic variation in the DO mice allows for the association of genetic variants with a phenotype, akin to human GWAS (17). The goal of our study was to identify the underlying genes responsible for the variation in urinary $Mg^{2+}$ excretion and thereby provide insight into the mechanism of changes in excretion with age. We therefore performed quantitative trait locus (QTL) analysis in mice at 6, 12, and 18 mo of age to find loci that could explain part of the variation in urinary $Mg^{2+}$ excretion at these different ages.

## MATERIALS AND METHODS

### Animals and Phenotypes in the Diversity Outbred Population

Our discovery cohort consisted of J:DO mice (JR No. 009376) from The Jackson Laboratory. Animals were maintained on pine shavings and given a rodent diet (LabDiet 5K12 with 0.23% wt/wt $Mg^{2+}$, St. Louis, MO) and acidified water in a room without pathogens. Spot urine was collected around 7:00 AM at 6, 12, and 18 mo of age. All animal experiments were performed in accordance with the National Institutes of Health Guide for the Care and Use of Laboratory Animals (National Research Council) and were approved by The Jackson Laboratory's Animal Care and Use Committee.

### Genetic Analysis in the Diversity Outbred Population

All mice were fully genotyped for 143,259 single-nucleotide polymorphisms (SNPs) using the Giga Mouse Universal Genotyping Array (GigaMUGA) built on an Illumina Infinium platform (GeneSeek, Neogen Genomics, Lincoln, NE). Founder haplotype mosaics were reconstructed using a Hidden Markov Model of array intensity data generated from Illumina's BeadStudio algorithm. QTL mapping in DO mice requires the use of a mixed-linear regression model accounting for kinship using the R/qtl2 R package (available from https://kbroman.org/qtl2) (18). R/qtl2 was used to calculate a QTL model (Mg $\sim$ sex + generation + cohort + ln(Cr + 10) + QTL), which accounted for sex, generation, and creatinine (Cr) as additive covariates for the urinary $Mg^{2+}$ phenotype. Used in conjunction with QTL mapping, R/qtl2 was also used to calculate SNP association with urinary $Mg^{2+}$ levels. LOD scores of individual SNPs under the QTL peaks of interest were calculated to further increase our resolution to the gene level.

### Generation and Characterization of *Oit3*$^{-/-}$ Mice

We deleted 803 base pairs in the *Oit3* gene including most of exon 2 using CRISPR/Cas9 with four guide RNAs in the 129S1/SvImJ mouse strain (Supplemental Fig. S1). For genotyping, gDNA was extracted from tail tips. Genotyping was performed using the following primers: ACATCACCGGCTATCTCTGG and TTTCTCATGGCTCAGGGACT with a standard PCR program and a 60°C annealing temperature (Supplemental Fig. S1). In addition, knockout was validated on mRNA level using liver tissue and primers spanning exons 2 and 3 (Supplemental Fig. S1). The newly developed *Oit3* knockout (*Oit3*$^{-/-}$) strain was designated *129S1/SvImJ-Oit3*$^{em1Rkor}$/RkorJ (JR No. 34668). Thirty-seven *Oit3*$^{-/-}$ mice and 47 littermate controls [wild type (WT)] were housed in standard cages in a temperature- and light-controlled room. At 12 wk of age, animals were moved from our standard LabDiet 5K12 diet to different $Mg^{2+}$-containing diets: either AIN-93M 5Z4K with 0.22% $Mg^{2+}$ (control diet; TestDiet, Richmond, IN) [$n = 23$ for WT (12 females and 11 males) and $n = 16$ for *Oit3*$^{-/-}$ (9 females and 7 males)] or a challenge with the AIN-93M 5Z4J with 0.02% $Mg^{2+}$ (low $Mg^{2+}$ diet; Richmond, IN) [$n = 24$ for WT (11 females and 13 males) and $n = 21$ for *Oit3*$^{-/-}$ (12 females and 9 males)] for 14 days. At the end of the diet, animals were housed in individual metabolic cages (Tecniplast, Buguggiate, Italy) with ad libitum access to food and drinking water to collect 24-h urine and feces. The next day, blood was collected (submental), mice were euthanized, and organs were collected.

### High-Fat, Low-$Mg^{2+}$ Mouse Study

Liver samples from a previously published experiment were used, in which mice were placed on a high-fat and low-$Mg^{2+}$ diet (19). In brief, 17-wk-old male C57BL6/J mice were placed on one of the following diets: normal $Mg^{2+}$ and low fat (0.21% wt/wt $Mg^{2+}$, 10% energy from palm oil), normal $Mg^{2+}$ and high fat (0.21% wt/wt $Mg^{2+}$, 60% energy from palm oil), low $Mg^{2+}$ and low fat (0.03% wt/wt $Mg^{2+}$ and 10% energy from palm oil), or low $Mg^{2+}$ and high fat (0.03% wt/wt $Mg^{2+}$ and 60% energy from palm oil) for 17 wk ($n = 12$/group). This study was approved by the animal ethics board of the Radboud University Nijmegen (RU DEC 2015-0073) and the Dutch Central Commission for Animal Experiments (CCD, AVD103002015239).

### Biochemical Measurements

Serum was isolated from blood by allowing it to clot for 20 min at room temperature followed by 20-min centrifugation (1,000 *g*). For the spot urine measurements in the DO mice, urinary $Mg^{2+}$ and creatinine concentrations were measured using a Synchron CX5 Chemistry Analyzer (Beckman Coulter AU680, Brea, CA). For the *Oit3*$^{-/-}$ mice, serum and urine $Mg^{2+}$ concentrations were measured with a Xylidyl Blue-I-based colorimetric assay according to the manufacturer's protocol (Roche Diagnostics, Rotkreuz, Switzerland), whereas serum and urine calcium ($Ca^{2+}$) concentrations were measured with a colorimetric assay as described previously (20). Feces was incubated in nitric acid (>65%, Sigma-Aldrich, Steinheim,

Germany) for 10 min at room temperature and subsequently incubated for 30 min at 50°C, followed by another 3-h incubation at room temperature. Fecal $Ca^{2+}$ and $Mg^{2+}$ concentrations were measured as described earlier. Urinary creatinine concentrations were measured using a Jaffé-based assay according to the manufacturer's protocol (Labor + Technik, Berlin, Germany), and serum creatinine concentrations were performed using an enzymatic assay according to the manufacturer's protocol (Crystal Chem, Inc., Elk Grove Village, IL). Fractional excretion of $Mg^{2+}$, i.e., the percentage of filtered $Mg^{2+}$ that is excreted in the urine, was calculated as: $\frac{[Mg^{2+}]_{urine} \times [Creatinine]_{serum}}{0.7 \times [Mg^{2+}]_{serum} \times [Creatinine]_{urine}} \times 100\%$ (21, 22). Serum triglyceride levels and urinary sodium ($Na^{+}$) and potassium ($K^{+}$) concentrations were measured in the Department of Laboratory Medicine of the Radboudumc.

### RNA Extraction, cDNA Synthesis, and qPCR

Kidneys and livers were snap-frozen in liquid nitrogen after isolation and stored at −80°C until total RNA extraction. RNA was extracted using TRIzol (Invitrogen, Carlsbad, CA) according to the manufacturer's protocol. Following DNAse treatment according to protocol (Promega, Madison, WI), cDNA was synthesized using Moloney murine leukemia virus reverse transcriptase (Invitrogen, Carlsbad, CA) using 1.5 μg total RNA. Then, qPCR was performed in triplicate for each sample using iQ SYBR Green (Bio-Rad, Hercules, CA) and specific primers (Supplemental Table S1). Data analysis was performed using the $2^{-\Delta\Delta Ct}$ method with *18s* rRNA for reference.

### Western Blotting

Urinary uromodulin excretion was determined by Western blotting. A urine volume equivalent to 3.75 nmol creatinine was prepared in Laemmli sample buffer [2% wt/vol sodium dodecyl sulfate (SDS)] (MP Biomedicals, Santa Ana, CA), 0.01% wt/vol bromophenol blue (Bio-Rad, Hercules, CA), 6% vol/vol glycerol (MP Biomedicals, Santa Ana, CA), and 50 mM Tris pH 6.8 [provided by the Laboratory Support & Media preparation group (LEM) of the Radboudumc] containing 100 mM dithiothreitol (MP Biomedicals, Santa Ana, CA) and protease inhibitors [174 μg/mL phenylmethylsulfonyl fluoride (Sigma-Aldrich, Steinheim, Germany), 1 μg/mL aprotinin (BioChemica, Darmstadt, Germany), 5 μg/mL leupeptin (MP Biomedicals, Santa Ana, CA), and 1 μg/mL pepstatin A (MP Biomedicals, Santa Ana, CA)] and incubated for 30 min at 37°C. Subsequently, urine samples were used for SDS-polyacrylamide gel electrophoresis on a 10% SDS gel and Western blotting as described previously (23). Goat anti-uromodulin (1:1,000 vol/vol; Cappel Research Reagents, Solon, OH; No. 55140) and peroxidase-conjugated rabbit anti-goat IgG (1:2,000 vol/vol; DakoCytomation Denmark A/S, Glostrup, Denmark; No. P044901) antibodies were used. Densitometry analysis was performed using ImageJ (National Institutes of Health, Bethesda, MD).

### Statistical Analyses

Statistical analyses were performed using R (Figs. 1, 2, 3, and 4) or GraphPad Prism 9 (other figures) (GraphPad software, San Diego, CA). Two-way ANOVA was used for testing the effect of two variables (e.g., diet and genotype); in case of a significant interaction term, Tukey's post hoc test was used. For all analyses, a $P$ value of $<0.05$ was considered statistically significant. Data are presented as means ± SE.

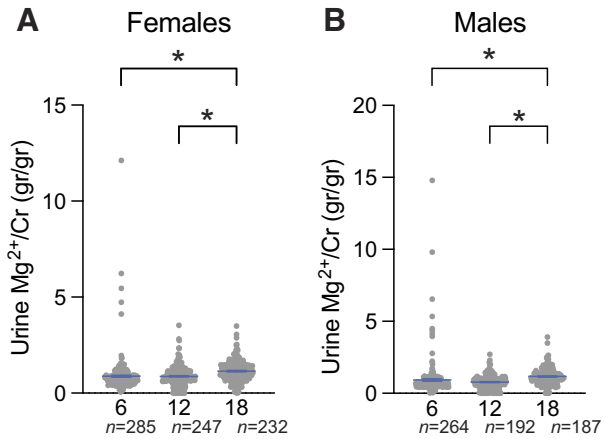


**Figure 1.** Increased urinary $Mg^{2+}$ excretion upon aging in mice. A significant increase in urinary $Mg^{2+}$ excretion was present after 18 mo of age compared with 6 and 12 mo of age in both female (*A*) and male (*B*) mice of the Diversity Outbred cohort. Data are shown as means ± SE. $*P < 0.05$ by one-way ANOVA with Tukey–Kramer post hoc test.

## RESULTS

### Urinary $Mg^{2+}$ Excretion Is Increased by Aging

To determine the effects of aging on urinary $Mg^{2+}$ excretion, we collected spot urine samples in a cohort of Diversity Outbred (DO) mice at 6 (353 females and 325 males), 12 (349 females and 299 males), and 18 mo (306 females and 260 males) of age. Unfortunately, the collected volume of spot urine was insufficient to measure both $Mg^{2+}$ and creatinine concentrations in several animals. For the samples that we could measure correctly (6 mo: 285 females and 264 males; 12 mo: 247 females and 192 males; 18 mo: 232 females and 187 males), a significant increase in urinary $Mg^{2+}$ excretion was observed on average in animals 18 mo of age compared with 6 and 12 mo of age (Fig. 1, *A* and *B*). For male mice, the average $Mg^{2+}$ to creatinine ratio increased from 0.77 to 1.17 between 12 and 18 mo of age, whereas for female mice, the average $Mg^{2+}$ to creatinine ratio increased from 0.87 to 1.14 between 12 and 18 mo of age.

### Association of Chromosomal Loci With Urinary $Mg^{2+}$ Excretion at Different Ages

We performed a genetic analysis on urinary $Mg^{2+}$ levels with the log-transformed creatinine levels and sex as an additive covariate at the three time points. The percent variance explained by genetics after accounting for covariates is 24.4%, 15.7%, and 25.1% at 6, 12, and 18 mo of age, respectively. At 6 mo, we observed a QTL on chromosome 10 that almost reached the 95% significance threshold (Fig. 2*A*). This peak was not present at 12 (Fig. 2*B*) and 18 mo of age (Fig. 2*C*). Instead, a peak on chromosome 19 was observed at 12 and 18 mo of age. This peak is above the 90% significance threshold but below the 95% significance threshold at 12 mo and is above the 95% significance threshold at 18 mo. The chromosome 19 locus by itself explains 2.92%, 4.93%, and

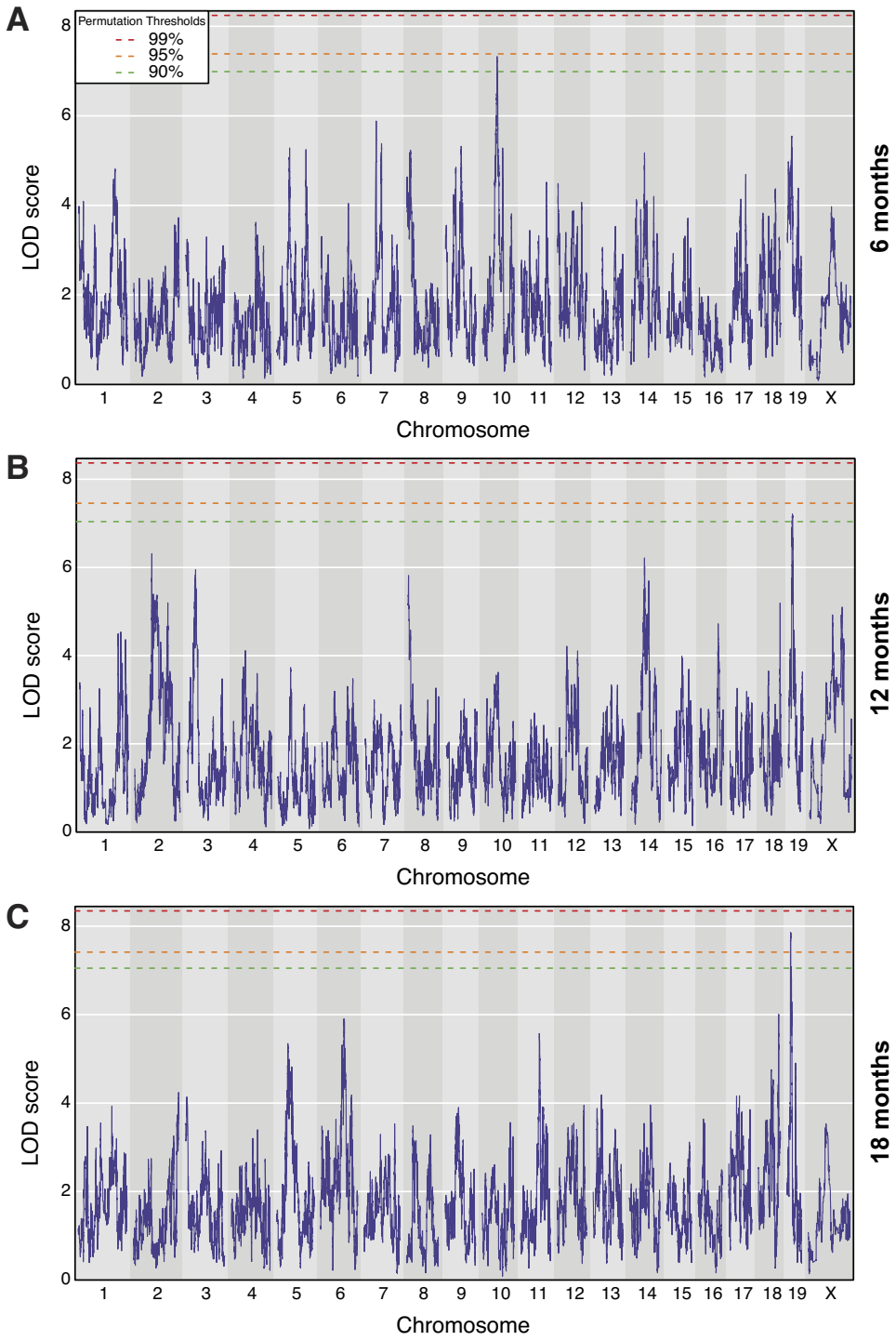


**Figure 2.** Quantitative trait locus (QTL) analysis for age-dependent $Mg^{2+}$ excretion. *A*: a QTL on chromosome 10 was associated with $Mg^{2+}$ excretion at 6 mo. *B*: at 12 mo, a QTL on chromosome 19 was associated with $Mg^{2+}$ excretion. *C*: the same QTL was also associated with $Mg^{2+}$ excretion at 18 mo.

7.59% of the variance at 6, 12, and 18 mo of age, respectively, and its contribution increases with age ($P = 0.0301$).

### Identification of *Oit3* as a Candidate Gene for Urinary $Mg^{2+}$ Excretion

The allele-effect plot shows that DO mice inheriting the locus on chromosome 10 from B6, 129, and WSB have high urinary $Mg^{2+}$ levels, whereas animals inheriting the locus from PWK and CAST have low urinary $Mg^{2+}$ levels (Fig. 3*A*). There were not enough animals in the cohort with A, NZO, and NOD alleles at this locus to determine their effect. The locus contains several genes, and we compared the genome sequences in the eight founder strains to look for variants that match the allele effect (B6 = 129 = WSB vs. PWK = CAST). The only SNP matching this pattern is *rs226054110*, which is in exon 5 of the *Oit3* gene. This SNP results in an amino acid substitution at position 243 of the protein: mice that inherited the *Oit3* allele from CAST and PWK founder strains have AAG (lysine), whereas mice that inherited the *Oit3* allele from any of the other five founder strains have GAG (glutamic acid)

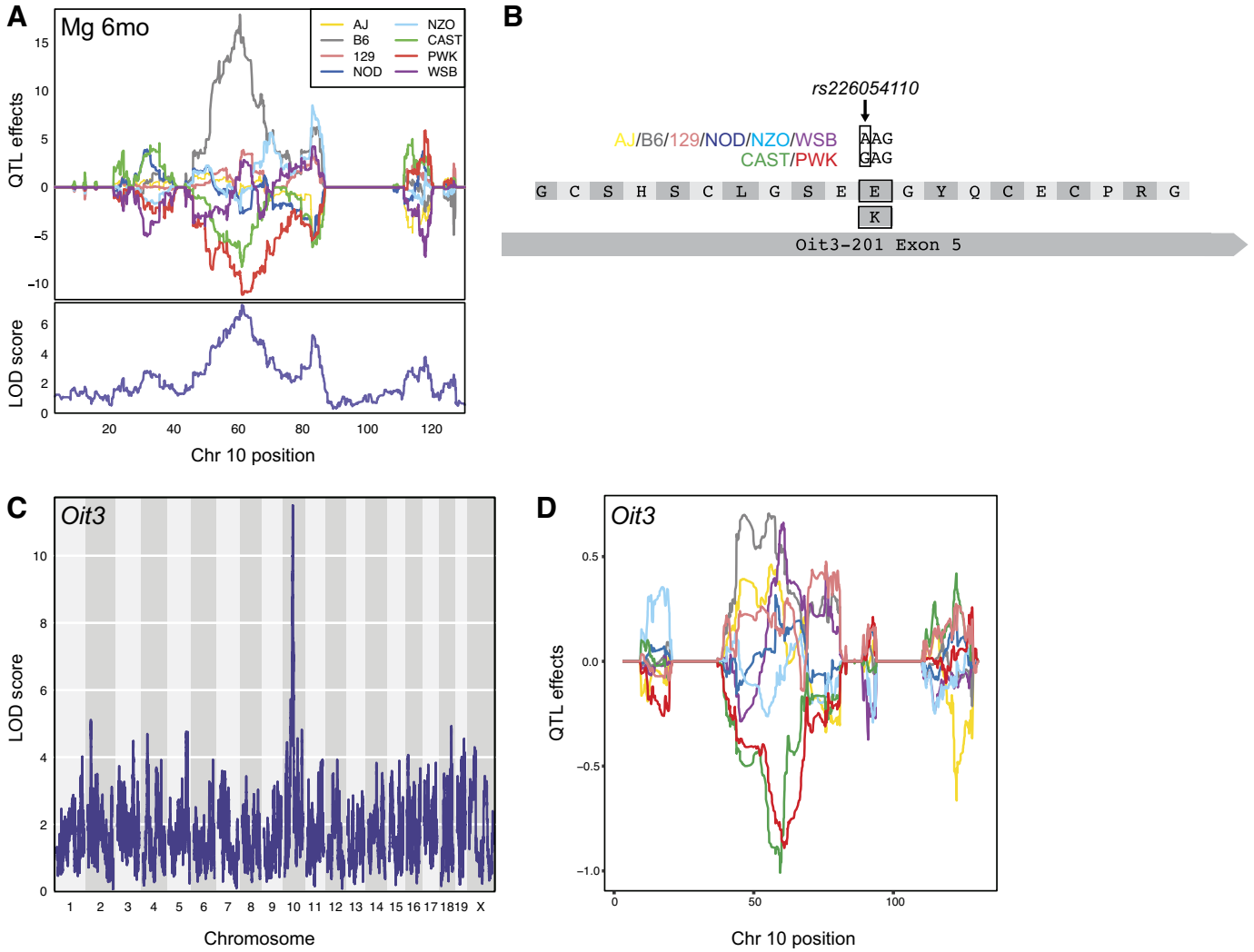


**Figure 3.** Allele-effect plots for quantitative trait locus (QTL) on chromosome 10. *A*: for the QTL on chromosome 10, mice inheriting alleles from B6, 129, and WSB have high urinary $Mg^{2+}$ levels compared with mice inheriting alleles from PWK and CAST. *B*: localization of single-nucleotide polymorphism (SNP) *rs226054110* in exon 5 of the *Oit3* gene, with mice inheriting alleles from CAST and PWK founder strains having glutamic acid (GAG) resulting in a lysine residue at protein position 243 and mice inheriting alleles from any of the other founder strains having GAG, resulting in a glutamic acid residue at this position. *C*: comparison of previously performed kidney RNA-Seq and eQTL data showed that *Oit3* expression was cis-regulated. *D*: mice inheriting alleles from the PWK and CAST strains had lower renal *Oit3* mRNA expression compared with the other strains.

(Fig. 3*B*). To consider the possibility that this SNP affects *Oit3* mRNA expression, we used previously published kidney RNAseq and expression QTL (eQTL) data from a subset of animals of this cohort (24). This showed that *Oit3* expression is cis-regulated (Fig. 3*C*), and the allele effect plot shows that the PWK and CAST alleles are associated with low *Oit3* expression (Fig. 3*D*). This matches the observed $Mg^{2+}$ QTL effects for the PWK and CAST alleles. OIT3 has been reported to be located in the renal tubule, and knockout leads to increased water, uric acid, and uromodulin excretion (25). Since uromodulin regulates renal $Mg^{2+}$ homeostasis through TPRM6 (26), we considered *Oit3* as a candidate gene worth exploring further.

## *Oit3*$^{-/-}$ Mice Have Unaltered Renal $Mg^{2+}$ Handling

To examine the role of *Oit3* in $Mg^{2+}$ excretion, we generated *Oit3*$^{-/-}$ mice using CRISPR/Cas9 technology. Interestingly, several attempts to generate the knockout in the C57BL/6J genetic background failed, whereas we had no problems generating the knockout in the 129S1/SvImJ background. WT and *Oit3*$^{-/-}$ mice were fed either a normal or a low-$Mg^{2+}$ diet for 14 days. No significant differences were present in the serum creatinine concentration or urine volume (Supplemental Fig. S2). For male mice, dietary $Mg^{2+}$ restriction resulted in a 20% decrease in serum $Mg^{2+}$ concentrations in both WT and *Oit3*$^{-/-}$ mice (Fig. 4*A*). A slight but statistically significant reduction of ~10% in serum $Mg^{2+}$ was present in male *Oit3*$^{-/-}$ mice compared with WT males for both the normal and the low-$Mg^{2+}$ diets (Fig. 4*A*). In contrast, although dietary $Mg^{2+}$ intake significantly reduced serum $Mg^{2+}$ by ~12% in female mice, no significant differences were present between female *Oit3*$^{-/-}$ mice and female WT mice (Fig. 5*A*). Urinary $Mg^{2+}$ excretion was significantly reduced in both WT and *Oit3*$^{-/-}$ male mice on a low-$Mg^{2+}$ diet, but no significant effect of genotype

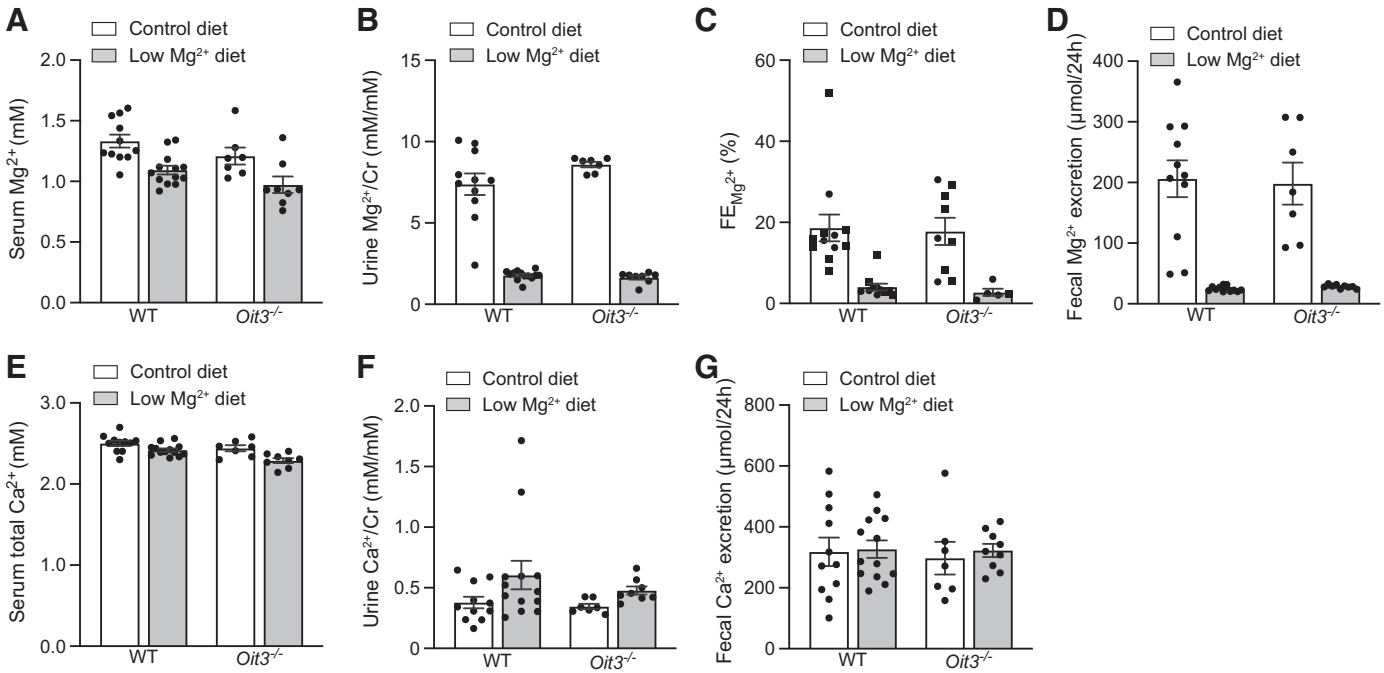


**Figure 4.** $Mg^{2+}$ homeostasis in male *Oit3*$^{-/-}$ mice. *A*: serum $Mg^{2+}$ levels were significantly lower in male *Oit3*$^{-/-}$ mice and upon a low-$Mg^{2+}$ diet ($P_{genotype}$ and $P_{diet} < 0.05$) ($n = 7–13$) . *B*: low dietary $Mg^{2+}$ content reduced urinary $Mg^{2+}$ excretion, but no effect of *Oit3*$^{-/-}$ was present ($P_{diet} < 0.0001$) ($n = 7–13$). *C*: fractional excretion of $Mg^{2+}$ ($FE_{Mg}{}^{2+}$) was significantly reduced on a low-$Mg^{2+}$ diet, but not affected by *Oit3* knockout ($P_{diet} < 0.0001$). Male mice are indicated by circles, female mice by squares ($n = 5–12$). *D*: fecal $Mg^{2+}$ excretion was not significantly different between male wild-type (WT) and *Oit3*$^{-/-}$ mice, but significantly reduced in animals on a low-$Mg^{2+}$ diet ($P_{diet} < 0.0001$) ($n = 7–12$). *E*: serum total $Ca^{2+}$ was significantly decreased by both *Oit3* knockout and low dietary $Mg^{2+}$ intake in male mice ($P_{genotype}$ and $P_{diet} < 0.05$) ($n = 7–13$). *F*: urinary $Ca^{2+}$ excretion was significantly higher in male mice on a low-$Mg^{2+}$ diet, but not significantly affected by *Oit3* knockout ($P_{diet} < 0.05$). *G*: no significant differences were present for $Ca^{2+}$ excretion between male WT and *Oit3*$^{-/-}$ mice or between animals fed a control diet or low $Mg^{2+}$ diet ($n = 7–13$). Data are shown as means ± SE and analyzed by two-way ANOVA.

was present (Fig. 4*B*). Similar results were obtained for female mice (Fig. 5*B*). A significant decrease in fractional excretion of $Mg^{2+}$ was also present for both genotypes on a low-$Mg^{2+}$ diet, but no differences were present between the two genotypes (Fig. 4*C*). Similarly, fecal $Mg^{2+}$ excretion was significantly decreased in male mice on a low-$Mg^{2+}$ diet, but no significant effects of genotype were present (Fig. 4*D*). Identical results were obtained for female WT and *Oit3*$^{-/-}$ mice (Fig. 5*C*). A significant reduction in serum total $Ca^{2+}$ levels was observed for male *Oit3*$^{-/-}$ mice compared with WT animals, whereas low dietary $Mg^{2+}$ also reduced the serum total $Ca^{2+}$ concentration (Fig. 4*E*). In contrast, serum $Ca^{2+}$ levels were not affected by genotype or diet in female mice (Fig. 5*D*). Low dietary $Mg^{2+}$ significantly increased urinary $Ca^{2+}$ excretion in male mice regardless of genotype (Fig. 4*F*). In contrast, a significant increase in urinary $Ca^{2+}$ excretion upon low dietary $Mg^{2+}$ was observed in female WT mice but not in female *Oit3*$^{-/-}$ mice (Fig. 5*E*). A significantly higher fecal $Ca^{2+}$ excretion was present in female *Oit3*$^{-/-}$ mice compared with female WT mice (Fig. 5*F*), but not in male mice (Fig. 4*G*). For male mice, urinary $Na^{+}$ excretion was not affected by genotype or diet. In contrast, low dietary $Mg^{2+}$ intake significantly increased urinary $Na^{+}$ excretion in female mice, although no effect of *Oit3* knockout was observed. In addition, a low-$Mg^{2+}$ diet increased urinary $K^{+}$ excretion in both male and female mice, without any significant effects of genotype in either sex (Supplemental Fig. S2).

### *Oit3* Knockout Does Not Affect the Expression of Genes Involved in Renal $Mg^{2+}$ Reabsorption

To determine whether *Oit3*$^{-/-}$ mice have altered expression of genes involved in renal $Mg^{2+}$ reabsorption, qPCR was performed. No significant differences were observed for *Cldn16* (Fig. 6*A*) and *Cldn19* (Fig. 6*B*), which are involved in paracellular $Mg^{2+}$ and $Ca^{2+}$ reabsorption in the thick ascending limb of Henle's loop (27), between male WT and *Oit3*$^{-/-}$ mice. However, a significant reduction in *Cldn19* expression was observed for both genotypes on a low-$Mg^{2+}$ diet (Fig. 6*B*). In contrast, no significant effects of diet or genotype on *Cldn16* and *Cldn19* expression were present in female mice (Fig. 7, *A* and *B*). Also, no significant differences by diet or genotype were observed in male mice for the expression of genes involved in transcellular $Mg^{2+}$ reabsorption in the distal convoluted tubule (DCT), including *Trpm6* (Fig. 6*C*), *Trpm7* (Fig. 6*D*), *Cnnm2* (Fig. 6*E*), *Pvalb* (Fig. 6*F*), *Slc41a1* (Fig. 6*G*), and *Slc41a3* (Fig. 6*H*) (28). Similar results were found for female mice (Fig. 7, *C–H*).

Furthermore, *Oit3*$^{-/-}$ also did not affect the expression of genes related to transcellular $Ca^{2+}$ reabsorption in male mice, including *Atp2b4* (encoding PMCA4), *Calb1* (encoding calbindin-$D_{28k}$), *Slc8a1* (encoding NCX1), and *Trpv5* (encoding TRPV5) (Fig. 8, *A–D*) (29). However, a significant decrease in *Slc8a1* (Fig. 8*C*) and *Trpv5* (Fig. 8*D*) was observed in both genotypes on a low-$Mg^{2+}$ diet. Similarly, no effects of *Oit3*$^{-/-}$ on renal calciotropic gene expression were observed in female

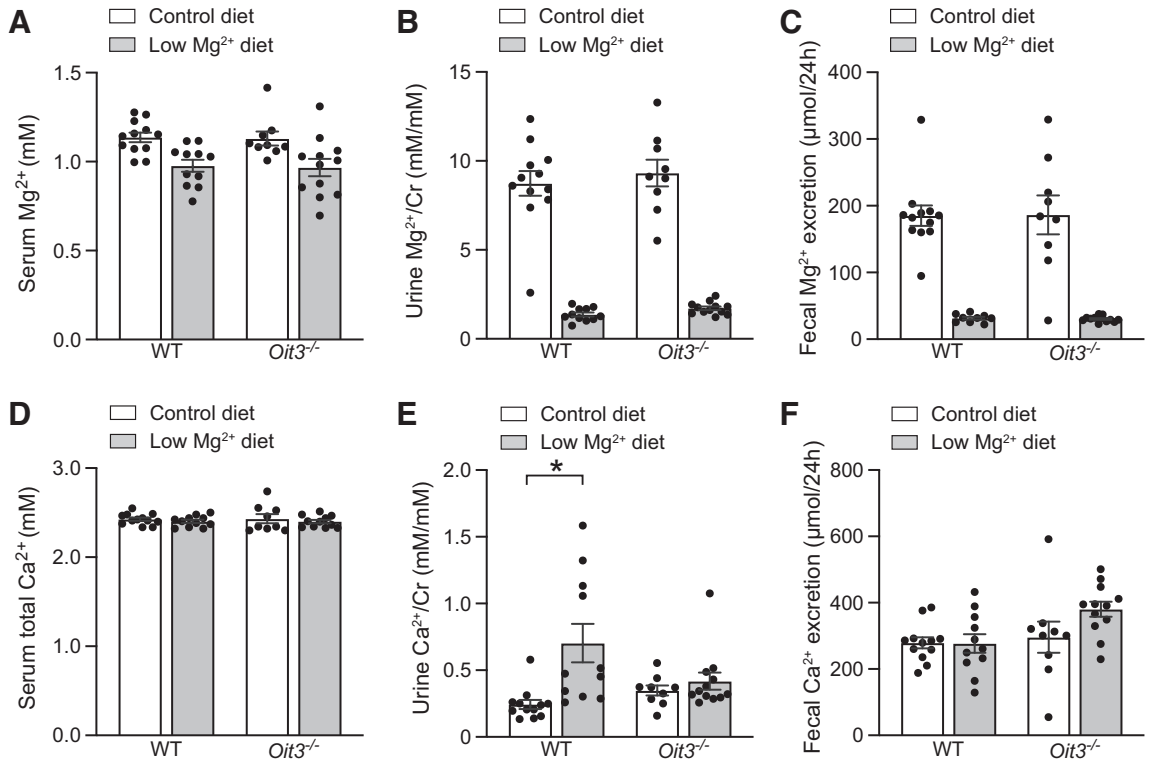


**Figure 5.** Serum, urinary, and fecal levels of $Mg^{2+}$ and $Ca^{2+}$ in female *Oit3*$^{-/-}$ mice. *A*: serum $Mg^{2+}$ levels were significantly decreased by low dietary $Mg^{2+}$ intake, but not affected by knockout of *Oit3* in female mice ($P_{diet} = 0.0002$) ($n = 9$–12). *B*: urinary $Mg^{2+}$ excretion was not significantly different between female WT and *Oit3*$^{-/-}$ mice, but significantly decreased by a low-$Mg^{2+}$ diet ($P_{diet} < 0.0001$) ($n = 9$–12). *C*: fecal $Mg^{2+}$ excretion was significantly decreased in female wild-type (WT) and *Oit3*$^{-/-}$ mice by low dietary $Mg^{2+}$, but no significant differences were present between the genotypes ($P_{diet} < 0.0001$) ($n = 9$–12). *D*: no significant differences in serum total $Ca^{2+}$ concentrations were present between any of the groups for female mice ($n = 9$–12) . *E*: low dietary $Mg^{2+}$ intake significantly increased urinary $Ca^{2+}$ excretion in female WT mice, but not in female *Oit3*$^{-/-}$ mice ($P_{diet} = 0.003$, $P_{interaction} = 0.03$) ($n = 9$–12). *F*: fecal $Ca^{2+}$ was significantly increased in female *Oit3*$^{-/-}$ mice, but not affected by a low-$Mg^{2+}$ diet ($P_{genotype} = 0.04$) ($n = 9$–12). Data are shown as means ± SE and analyzed by two-way ANOVA. *$P < 0.05$ by two-way ANOVA with Tukey's post hoc test.

mice (Fig. 9, *A*–*D*). Low dietary $Mg^{2+}$ did significantly reduce *Slc8a1* expression in both genotypes compared with the control diet (Fig. 9*C*).

As OIT3 has previously been reported to increase urinary uromodulin excretion (25), urinary uromodulin levels were also determined using immunoblotting. However, urinary uromodulin excretion was not significantly altered in male *Oit3*$^{-/-}$ mice or female *Oit3*$^{-/-}$ mice (Supplemental Fig. S3).

### *Oit3* Knockout Does Not Affect Serum Triglyceride Levels

OIT3 is highly expressed in the liver, and previous studies in C57BL/6J mice have shown that OIT3 is involved in triglyceride release (30–32). We did not observe any difference in serum triglyceride levels between our WT and *Oit3*$^{-/-}$ mice, which are on the 129S1/SvImJ genetic background. In addition, hepatic *Oit3* expression was previously found to be increased on a high-fat diet (31). To test whether the expression of *Oit3* in the liver was affected by dietary fat intake and/or low-$Mg^{2+}$ intake, samples from a previously published study in C57BL/6J mice were used (19). However, neither high-fat intake nor low-$Mg^{2+}$ intake affected the expression of *Oit3* (Supplemental Fig. S4).

### Association of Trpm6 With Urinary $Mg^{2+}$ Excretion at 12 and 18 mo of Age

We also further investigated the chromosome 19 locus associated with urinary $Mg^{2+}$ excretion in DO mice 12 and 18 mo of age. This coincided with the location of *Trpm6*, a gene that has been shown to play an important role in $Mg^{2+}$ reabsorption in the DCT. The allele-effect plot for the chromosome 19 locus showed that DO mice inheriting alleles from the CAST, NOD, A, WSB, and B6 founder strains have higher urinary $Mg^{2+}$ levels than DO mice inheriting alleles from the 129, NZO, and PWK founder strains (Fig. 10*A*). Analyzing the genome sequences of the eight founder strains, we did not see any variant in the exons that matched this pattern, suggesting the variation in urinary $Mg^{2+}$ levels was not caused by a coding variant in *Trpm6*. We used previously published kidney RNAseq and eQTL data from a subset of animals of our cohort (24) to determine whether *Trpm6* is cis-regulated and whether the cis-eQTL allele-effect pattern matches the allele effect pattern of our $Mg^{2+}$ QTL. Indeed, *Trpm6* expression variation in the DO is mostly determined by a cis-eQTL at the *Trpm6* locus (Fig. 10*B*) and the allele effect plot of this eQTL is opposite of the $Mg^{2+}$ QTL except for the CAST and 129 alleles (Fig. 10*C*).

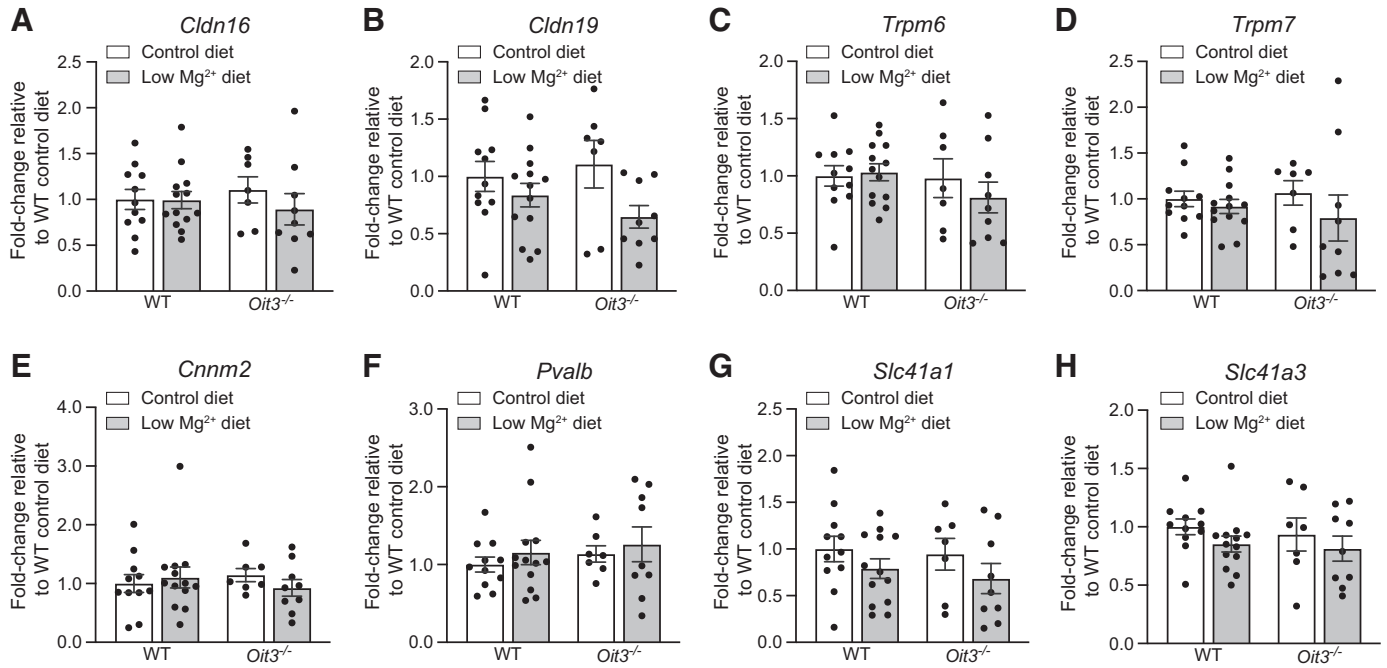


**Figure 6.** Male *Oit3*$^{-/-}$ mice have unaltered expression of genes involved in renal $Mg^{2+}$ reabsorption. *A*: *Cldn16* expression was unaltered by *Oit3* knockout or low dietary $Mg^{2+}$ intake in male mice ($n = 7$–13). *B*: low dietary $Mg^{2+}$ significantly decreased *Cldn19* expression, but no significant effects of genotype were present ($P_{diet} < 0.05$) ($n = 7$–13). *C*: *Trpm6* expression was not affected by diet or *Oit3* knockout ($n = 7$–13). *D*: *Trpm7* expression was also unaffected by diet or genotype ($n = 7$–13). *E*: the expression of *Cnnm2* was not affected by low $Mg^{2+}$ intake or knockout of *Oit3* ($n = 7$–13). *F*: no significant differences in *Pvalb* expression were present between the different groups ($n = 7$–13). *G*: *Slc41a1* expression was unaltered by low $Mg^{2+}$ intake or *Oit3* knockout ($n = 7$–13). *H*: *Slc41a3* expression was also not affected by diet or genotype ($n = 7$–13). Data are shown as means ± SE and analyzed by two-way ANOVA. WT, wild type.

## DISCUSSION

In this study, we demonstrate that urinary $Mg^{2+}$ excretion is increased during aging in a large cohort of genetically diverse mice. Our genetic analyses identified two loci that are associated with $Mg^{2+}$ excretion: a locus on chromosome 10 at 6 mo of age and a locus on chromosome 19, containing the gene encoding the $Mg^{2+}$ channel TRPM6, at 12 and 18 mo of age.

For the chromosome 10 locus, we identified only one SNP consistent with the allele-effect plot for urinary $Mg^{2+}$ excretion at age 6 mo, which is in exon 5 of *Oit3*. OIT3 (or liver-specific zona pellucida domain-containing protein; LZP) is a 60-kDa-sized protein expressed in the liver (30, 32–34). Immunohistochemistry has demonstrated renal OIT3 protein expression in the thick ascending limb of Henle's loop, whereas OIT3 has also been implicated in tubular uric acid reabsorption (25, 33). In addition, experiments showed that OIT3 is secreted and is detectable in urine (33, 34). In contrast, recent (single-cell) RNA sequencing experiments suggest negligible *Oit3* mRNA expression in the kidney (35–37). These results were further supported by a recent study using lineage tracing, which also confirmed no *Oit3* expression in the kidneys (38). It is possible that a certain stimulus, which was present in the previous study that generated *Oit3*$^{-/-}$ mice but absent in the RNA sequencing studies, is required to induce renal *Oit3* mRNA expression. In addition, differences in genetic background between the 129S1/SvImJ used to generate the *Oit3*$^{-/-}$ mice and the C57BL/6 strain used for RNAseq might affect results (25, 35). The SNP in exon 5 of *Oit3* (*rs226054110*) leads to an amino acid change [mice with the CAST or PWK alleles have AAG (lysine), the other alleles have GAG (glutamic acid)] and is associated with differences in *Oit3* expression in a subset of our cohort. Further elucidation of OIT3 function is required to test the effects of this SNP. However, as the molecular function of OIT3 remains to be elucidated, a clear readout for assessing the consequences of this SNP is currently lacking.

As OIT3 was reported to be expressed in the TAL (25), which is the segment where the majority of the filtered $Mg^{2+}$ is reabsorbed (50–70%) (1), this would make it a promising regulator of urinary $Mg^{2+}$ excretion. However, urinary $Mg^{2+}$ excretion was unchanged in the *Oit3*$^{-/-}$ mice generated in our study, even when the mice were challenged with a low-$Mg^{2+}$ diet. We did observe a mild but significant decrease of ~0.1 mM in serum $Mg^{2+}$ concentrations in *Oit3*$^{-/-}$ mice compared with WT mice on either the control or low-$Mg^{2+}$ diet, although this effect was restricted to male animals. A significantly lower serum $Ca^{2+}$ concentration was found in male *Oit3*$^{-/-}$ mice compared with WT male mice regardless of diet. This effect was again not present in female *Oit3*$^{-/-}$ mice. These changes in serum $Mg^{2+}$ and $Ca^{2+}$ concentrations in male *Oit3*$^{-/-}$ mice are likely not caused by altered renal or intestinal $Mg^{2+}$ and $Ca^{2+}$ handling, given the unaltered urinary and fecal excretion of these electrolytes. Moreover, we did not observe any differences in the expression of key magnesiotropic and calciotropic genes in the kidneys of male *Oit3*$^{-/-}$ mice. Although the mechanism underlying these sex differences remains to be elucidated, OIT3 expression has been detected in testes (33). In addition,

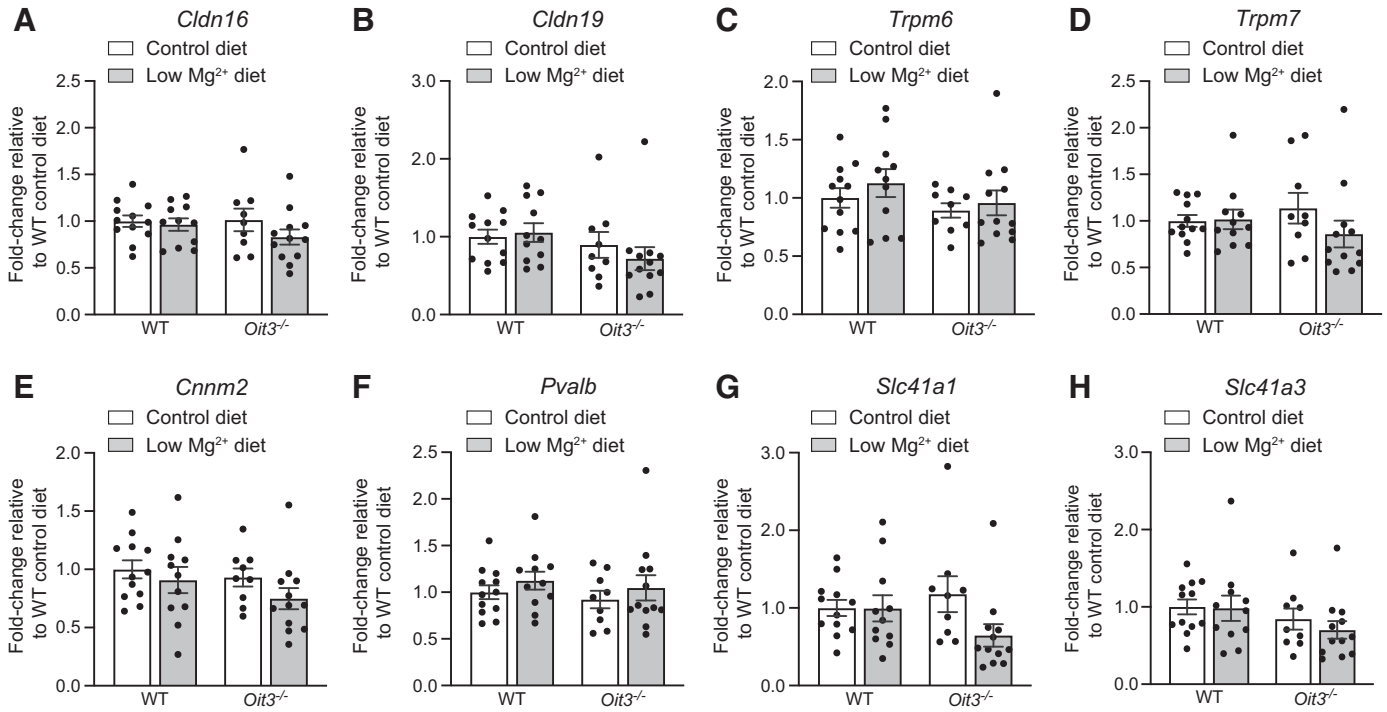


**Figure 7.** Expression of magnesiotropic genes in kidneys of female *Oit3*$^{-/-}$ mice. *A*: *Cldn16* expression was similar in all groups ($n$ = 9–12). *B*: *Cldn19* expression was also not affected by low dietary $Mg^{2+}$ or *Oit3* knockout ($n$ = 9–12). *C*: no significant differences in *Trpm6* expression were present between any of the groups ($n$ = 9–12). *D*: the expression of *Trpm7* was also not affected by diet or genotype ($n$ = 9–12). *E*: no significant differences in *Cnnm2* expression were present between the diets and the genotypes ($n$ = 9–12). *F*: *Pvalb* expression was not significantly affected by a low-$Mg^{2+}$ diet or *Oit3* knockout ($n$ = 9–12). *G*: low dietary $Mg^{2+}$ or knockout of *Oit3* did not affect the expression of *Slc41a1* ($n$ = 9–12). *H*: *Slc41a3* expression was similar between the 4 groups ($n$ = 9–12). Data are shown as means ± SE and analyzed by two-way ANOVA. WT, wild type.

*Oit3* mRNA expression in sperm was associated with fertility in bulls (39). We thus speculate that OIT3 knockout, perhaps through interfering with the release of testosterone, might interfere with serum $Mg^{2+}$ levels. Further studies are required to formally address this hypothesis and the underlying mechanism.

As the PWK/CAST allele is associated with lower *Oit3* gene expression and lower urinary $Mg^{2+}$ excretion, it is possible that increased *Oit3* gene expression could increase urinary $Mg^{2+}$ excretion. In line with the minimal *Oit3* expression under baseline conditions, *Oit3* expression could be increased in the case of increased dietary $Mg^{2+}$ intake to enhance urinary $Mg^{2+}$ excretion. Follow-up experiments using a high-$Mg^{2+}$ diet should be performed to investigate this hypothesis.

The unaltered urinary excretion of $Mg^{2+}$ in *Oit3*$^{-/-}$ mice fits with a barely detectable mRNA expression of *Oit3* in the kidneys of C57BL/6 mice (35). An interesting observation is that several attempts to generate a knockout allele in C57BL/6J failed and we therefore decided to use the 129S1/SvImJ inbred strain instead. Thus, we cannot rule out strain-specific expression patterns of *Oit3*. In addition, although OIT3 is known to be secreted into the blood (32), its expected size of 60 kDa means it is unlikely to pass the glomerular filtration barrier. Of note, the highest expression of OIT3 was

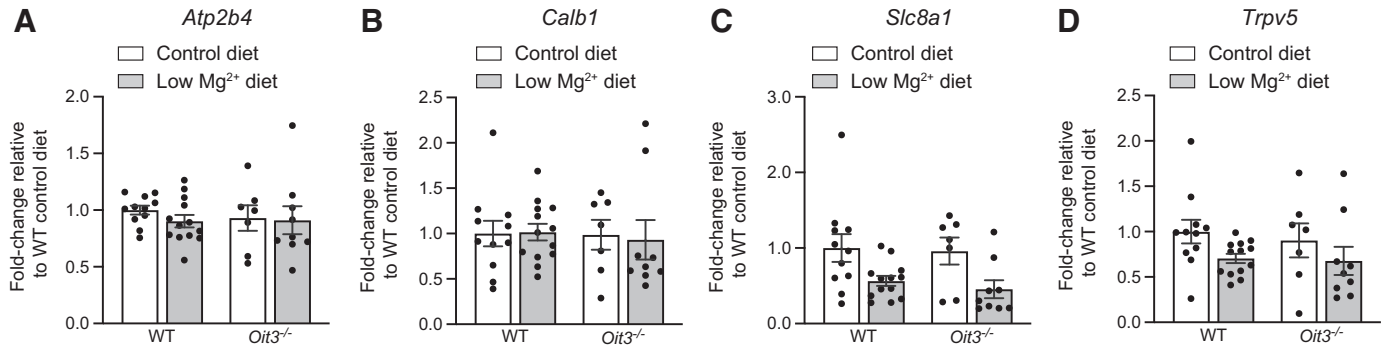


**Figure 8.** Expression of genes involved in transcellular $Ca^{2+}$ reabsorption in male *Oit3*$^{-/-}$ mice. *A*: *Atp2b4* expression was similar in all groups ($n$ = 7–13). *B*: low dietary $Mg^{2+}$ or *Oit3* knockout did not affect *Calb1* expression ($n$ = 7–13). *C*: a low-$Mg^{2+}$ diet significantly decreased *Slc8a1* expression, whereas no significant differences were present between wild-type (WT) and *Oit3*$^{-/-}$ mice ($P_{diet} < 0.05$) ($n$ = 7–13). *D*: *Trpv5* expression was significantly decreased by a low-$Mg^{2+}$ diet, but not affected by genotype ($P_{diet} < 0.05$) ($n$ = 7–13). Data are shown as means ± SE and analyzed by two-way ANOVA.

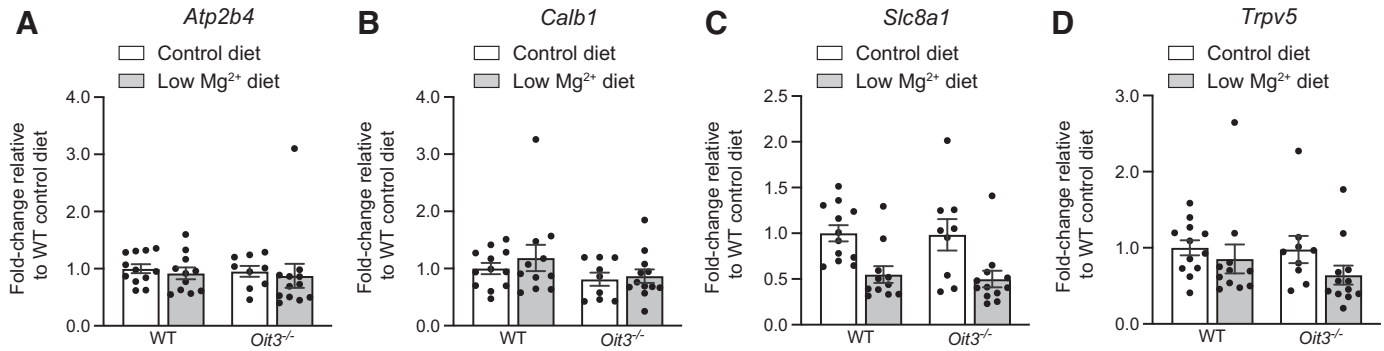


**Figure 9.** Expression of genes involved in transcellular $Ca^{2+}$ reabsorption in female *Oit3*$^{-/-}$ mice. *A*: *Atp2b4* expression was similar in all groups ($n = 9$–12). *B*: *Calb1* expression was also not significantly affected by a low-$Mg^{2+}$ diet or *Oit3* knockout ($n = 9$–12). *C*: *Slc8a1* expression was significantly decreased by a low-$Mg^{2+}$ diet, but not affected by genotype ($P_{diet} < 0.05$) ($n = 9$–12). *D*: no significant differences were present in *Trpv5* expression between any of the groups ($n = 9$–12). Data are shown as means ± SE and analyzed by two-way ANOVA. WT, wild type.

found in the liver (30, 32–34). In line with an important function of OIT3 in liver function, previous studies showed that *Oit3*$^{-/-}$ mice have reduced serum triglyceride levels due to impaired hepatic secretion (31). In addition, this study showed an increase in *Oit3* expression in the liver upon a high-fat diet (60%). Although serum triglyceride levels were unaltered in our *Oit3*$^{-/-}$ mice, it should be noted that we used a lower dietary fat content in our standard chow diet (6% wt/wt) compared with the previously published study (10% wt/wt). However, we did not observe *Oit3* upregulation in the livers of mice treated with a high-fat diet (60% wt/wt) (19). It is possible that differences in the duration of the high-fat diet (19 wk in our study compared with 10 wk in the previous study) provide an explanation for this difference. Importantly, a recent study also indicated that *Oit3* is mainly expressed in sinusoidal endothelial cells in the liver and only minimally in hepatocytes (38). Clearly, the role of OIT3 in the liver also requires further investigation.

As we could not confirm the role of OIT3 in $Mg^{2+}$ homeostasis using *Oit3*$^{-/-}$ mice, we cannot exclude the fact that other genes within the 95% confidence interval of the chromosome 10 locus could explain the association with urinary $Mg^{2+}$ excretion. For example, *Mcu* and *Micu1* are genes that encode mitochondrial $Ca^{2+}$ uniporters (40, 41). Given the link between mitochondrial dysfunction and hypomagnesemia (42, 43), it is possible that these genes affect $Mg^{2+}$ reabsorption in the kidney. Although *Mcu* and *Micu1* are ubiquitously expressed in the tubular system (35), the DCT has the highest mitochondrial density compared with other segments (44, 45). Thus, genetic variants in *Mcu* or *Micu1* might contribute to variation in urinary $Mg^{2+}$ excretion by affecting mitochondrial function in especially the DCT. Moreover, according to the UCSC Genome Browser (GRCm38/mm10), our SNP (*rs226054110*) is within an enhancer region in the genome (46). Hence, it could also affect the expression of other genes on chromosome 10.

Interestingly, a low-$Mg^{2+}$ diet increased urinary $Ca^{2+}$ excretion in both WT and *Oit3*$^{-/-}$ male mice, whereas for female mice this effect was absent in *Oit3*$^{-/-}$ mice. Other studies using low-$Mg^{2+}$ diets have reported inconsistent changes in urinary $Ca^{2+}$ excretion, with either a decreased (47–50) or unchanged urinary $Ca^{2+}$ excretion (51, 52). To the best of our knowledge, this is the first study showing increased urinary $Ca^{2+}$ excretion upon low dietary $Mg^{2+}$ intake. Given that most of these studies were performed on C57BL/6 mice, this points toward a differential effect of low-

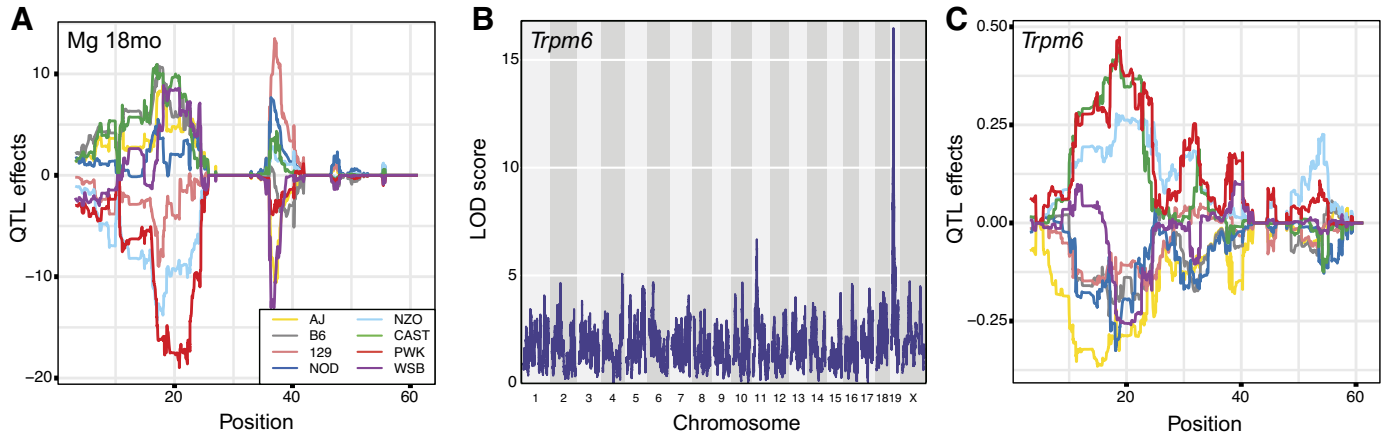


**Figure 10.** Allele-effect plots for quantitative trait locus (QTL) on chromosome 19. *A*: for the QTL on chromosome 19, mice inheriting alleles from CAST, NOD, AJ, WSB, and B6 have higher urinary $Mg^{2+}$ excretion than mice inheriting alleles from 129, NZO, and PWK mice. *B*: *Trpm6* expression variation in the Diversity Outbred (DO) mice is mostly determined by a cis-eQTL at the *Trpm6* locus. *C*: comparison of RNA-Seq and eQTL data showed that the expression of *Trpm6*, which is present on this locus, is negatively correlated to the QTL for $Mg^{2+}$ excretion.

$Mg^{2+}$ diet in 129S1/SvImJ mice. It is known, however, that severe hypomagnesemia reduces the secretion of parathyroid hormone (PTH) from the parathyroid gland (53–56). Given that PTH is an important stimulator of $Ca^{2+}$ reabsorption in the kidney, directly or by stimulating the formation of active vitamin D, it is possible that this explains the low-$Mg^{2+}$ diet-induced hypercalciuria (57). However, the low-$Mg^{2+}$ diet-induced hypomagnesemia in the current study is relatively modest and might not be sufficient to interfere with PTH release. Regardless of a possible involvement of PTH, a decrease in the expression of the apical $Ca^{2+}$ channel *Trpv5* was found in male mice (both WT and *Oit3*$^{-/-}$ mice), whereas in both male and female mice on a low-$Mg^{2+}$ diet a decrease in the basolateral $Na^+/Ca^{2+}$ exchanger NCX1 was observed. This likely results in decreased transcellular $Ca^{2+}$ reabsorption in the DCT/connecting tubule (58, 59).

We also found that low dietary $Mg^{2+}$ intake was associated with increased urinary $Na^+$ excretion in female mice, but not in male mice. Although the underlying mechanism remains to be determined, downregulation of the $Na^+$-$Cl^-$ cotransporter (NCC) in the DCT might be involved (60). Intriguingly, differences in DCT length and NCC expression have previously been identified between male and female mice (61), which could contribute to the female-specific natriuretic response following low dietary $Mg^{2+}$ intake. We also found a significant increase in urinary $K^+$ excretion following low dietary $Mg^{2+}$ intake in both male and female mice. As $Mg^{2+}$ inhibits $K^+$ secretion by inhibiting the renal outer medullary $K^+$ channel (ROMK) (62, 63), we hypothesize that reduced $Mg^{2+}$-dependent ROMK inhibition could contribute to the increased urinary $K^+$ excretion.

We show that genetic variation in a locus containing *Trpm6* contributed to the variation in urinary $Mg^{2+}$ excretion in mice aged 12 and 18 mo. *TRPM6* has been associated with serum $Mg^{2+}$ concentration and urinary $Mg^{2+}$ excretion in genome-wide association studies in a variety of cohorts, including healthy individuals, patients with diabetes, and users of proton pump inhibitors (13–16, 64, 65). Our observation that the allele-effect plot of *Trpm6* gene expression inversely correlated with the allele-effect plot for $Mg^{2+}$ excretion suggests that mice with lower *Trpm6* expression have higher urinary $Mg^{2+}$ excretion. This illustrates the important role of TRPM6 in renal $Mg^{2+}$ reabsorption, which is in line with the observed hypomagnesemia and hypermagnesiuria in a kidney-specific *Trpm6*$^{-/-}$ mouse model (66). The association with $Mg^{2+}$ excretion in our study was only present at 12 and 18 mo. This could indicate that decreased *Trpm6* mRNA expression might be involved in age-dependent increases in urinary $Mg^{2+}$ excretion. SNPs in *TRPM6* have also been associated with diabetes mellitus type 2 and insulin resistance (65, 67, 68). Given that insulin sensitivity is decreased upon aging and insulin increases TRPM6 channel activity (67, 69), SNPs in *Trpm6* might associate with urinary $Mg^{2+}$ excretion by altering insulin sensitivity, especially in aging mice. In addition, estrogen signaling has previously been linked to TRPM6 channel activity in vitro (70). As serum estradiol levels already decline in mice aged 12 mo (71), this could also contribute to the observed association of *Trpm6* with urinary $Mg^{2+}$ excretion at 12 and 18 mo of age. Moreover, we also did not determine whether TRPM6 channel activity or expression is altered during aging. As *Trpm6* is also responsible for colonic $Mg^{2+}$ absorption (49, 72), age-related changes in TRPM6-dependent $Mg^{2+}$ transport could also extend to other organs. Future studies should therefore address these open questions.

A limitation of our approach is that spot urine collections were used for measuring urinary $Mg^{2+}$ excretion in our large cohort DO mice. To correct for differences in hydration status, we measured urinary creatinine concentrations and used the log-transformed values (as they were non-normal distributed) as a covariate in our model for the genetic analysis. As creatinine is byproduct of muscle metabolism, its concentrations might be reduced to reduce muscle mass in aging mice. Nevertheless, mice might not yet exhibit loss of muscle mass at 18 mo of age (73), indicating that it could still be an appropriate normalization factor in our studies. However, creatinine is also secreted by the proximal tubule (up to 35%–50% of the total excreted creatinine) (74). To confirm that urinary $Mg^{2+}$ excretion is increased during aging, future studies should determine fractional urinary $Mg^{2+}$ excretion in 24-h urine using exogenous clearance markers (e.g., using inulin). This approach will also reveal whether urinary $Mg^{2+}$ excretion is increased due to altered renal $Mg^{2+}$ handling or reflects alterations in gastrointestinal $Mg^{2+}$ absorption. Given the discrepancies between our study and previous studies with regard to *Oit3*, which could be caused by differences in genetic background, age, or environmental conditions (e.g., diet), further studies are needed but were outside the scope of the current study.

In conclusion, we show that genetic variants in *Oit3* and *Trpm6* are associated with urinary $Mg^{2+}$ excretion in mice at distinct periods of life. However, *Oit3*$^{-/-}$ mice do not demonstrate defects in renal $Mg^{2+}$ handling.

## DATA AVAILABILITY

All data presented in the current study, as well as the raw data, are available upon reasonable request to the corresponding author.

## SUPPLEMENTAL DATA

Supplemental Fig. S1: https://doi.org/10.6084/m9.figshare.25817161.v1; Supplemental Fig. S2: https://doi.org/10.6084/m9.figshare.25817173.v1; Supplemental Fig. S3: https://doi.org/10.6084/m9.figshare.25817179.v1; Supplemental Fig. S4: https://doi.org/10.6084/m9.figshare.25817176.v1.

## ACKNOWLEDGMENTS

The authors thank Teun van Houtert, Caro Bos, Maria Ibars Serra, Alicia Warren, and Samantha Spellacy for expert technical assistance and JAX Genome Engineering Technologies for the generation of the *Oit3* knockout strain.

## GRANTS

This work was supported by National Institutes of Health Grant P30AG038070 (to R.K. and G.A.C.), a Radboud Institute for Molecular Life Sciences Research Grant (to J.H.), and a PhD research grant from the Radboud Institute for Molecular Life Sciences within the Radboud University Medical Center (to W.H.v.M.).

## DISCLOSURES

No conflicts of interest, financial or otherwise, are declared by the authors.

## AUTHOR CONTRIBUTIONS

R.K. conceived and designed research; W.H.v.M., O.D., and R.K. performed experiments; W.H.v.M., G.A.C., and R.K. analyzed data; W.H.v.M., G.A.C., and R.K. interpreted results of experiments; W.H.v.M. and R.K. prepared figures; W.H.v.M. and R.K. drafted manuscript; J.H.F.d.B., G.A.C., J.G.J.H., and R.K. edited and revised manuscript; W.H.v.M., J.H.F.d.B., G.A.C., J.G.J.H., and R.K. approved final version of manuscript.

## REFERENCES


1. **de Baaij JH**, **Hoenderop JG**, **Bindels RJ.** Magnesium in man: implications for health and disease. *Physiol Rev* 95: 1–46, 2015. doi:10.1152/physrev.00012.2014.
2. **Barbagallo M**, **Belvedere M**, **Dominguez LJ.** Magnesium homeostasis and aging. *Magnes Res* 22: 235–246, 2009. doi:10.1684/mrh.2009.0187.
3. **Gautam S**, **Khapunj A.** Prevalence of hypomagnesemia among elderly patients attending a tertiary care center: a descriptive cross-sectional study. *J Nepal Med Assoc* 59: 35–38, 2021. doi:10.31729/jnma.5764.
4. **Gullestad L**, **Nes M**, **Rønneberg R**, **Midtvedt K**, **Falch D**, **Kjekshus J.** Magnesium status in healthy free-living elderly Norwegians. *J Am Coll Nutr* 13: 45–50, 1994. doi:10.1080/07315724.1994.10718370.
5. **Yang XY**, **Hosseini JM**, **Ruddel ME**, **Elin RJ.** Blood magnesium parameters do not differ with age. *J Am Coll Nutr* 9: 308–313, 1990. doi:10.1080/07315724.1990.10720385.
6. **Ford ES**, **Mokdad AH.** Dietary magnesium intake in a national sample of US adults. *J Nutr* 133: 2879–2882, 2003. doi:10.1093/jn/133.9.2879.
7. **Petri M**, **Cumber P**, **Grimes L**, **Treby D**, **Bryant R**, **Rawlins D**, **Ising H.** The metabolic effects of thiazide therapy in the elderly: a population study. *Age Ageing* 15: 151–155, 1986. doi:10.1093/ageing/15.3.151.
8. **Coudray C**, **Feillet-Coudray C**, **Rambeau M**, **Tressol JC**, **Gueux E**, **Mazur A**, **Rayssiguier Y.** The effect of aging on intestinal absorption and status of calcium, magnesium, zinc, and copper in rats: a stable isotope study. *J Trace Elem Med Biol* 20: 73–81, 2006. doi:10.1016/j.jtemb.2005.10.007.
9. **Kołbuc M**, **Leßmeier L**, **Salamon-Słowińska D**, **Małecka I**, **Pawlaczyk K**, **Walkowiak J**, **Wysocki J**, **Beck BB**, **Zaniew M.** Hypomagnesemia is underestimated in children with HNF1B mutations. *Pediatr Nephrol* 35: 1877–1886, 2020. doi:10.1007/s00467-020-04576-6.
10. **Hunter DJ**, **Lange M. D**, **Snieder H**, **MacGregor AJ**, **Swaminathan R**, **Thakker RV**, **Spector TD.** Genetic contribution to renal function and electrolyte balance: a twin study. *Clin Sci (Lond)* 103: 259–265, 2002. doi:10.1042/cs1030259.
11. **Lieske JC**, **Turner ST**, **Edeh SN**, **Smith JA**, **Kardia SL.** Heritability of urinary traits that contribute to nephrolithiasis. *Clin J Am Soc Nephrol* 9: 943–950, 2014. doi:10.2215/CJN.08210813.
12. **Moulin F**, **Ponte B**, **Pruijm M**, **Ackermann D**, **Bouatou Y**, **Guessous I**, **Ehret G**, **Bonny O**, **Pechère-Bertschi A**, **Staessen JA**, **Paccaud F**, **Martin P-Y**, **Burnier M**, **Vogt B**, **Devuyst O**, **Bochud M.** A population-based approach to assess the heritability and distribution of renal handling of electrolytes. *Kidney Int* 92: 1536–1543, 2017. doi:10.1016/j.kint.2017.06.020.
13. **Corre T**, **Arjona FJ**, **Hayward C**, **Youhanna S**, **de Baaij JHF**, **Belge H et al.** Genome-wide meta-analysis unravels interactions between magnesium homeostasis and metabolic phenotypes. *J Am Soc Nephrol* 29: 335–348, 2018. doi:10.1681/ASN.2017030267.
14. **Meyer TE**, **Verwoert GC**, **Hwang S-J**, **Glazer NL**, **Smith AV**, **van Rooij FJA et al.** Genome-wide association studies of serum magnesium, potassium, and sodium concentrations identify six loci influencing serum magnesium levels. *PLoS Genet* 6: e1001045, 2010. doi:10.1371/journal.pgen.1001045.
15. **Tin A**, **Köttgen A**, **Folsom AR**, **Maruthur NM**, **Tajuddin SM**, **Nalls MA**, **Evans MK**, **Zonderman AB**, **Friedrich CA**, **Boerwinkle E**, **Coresh J**, **Kao WHL.** Genetic loci for serum magnesium among African-Americans and gene-environment interaction at MUC1 and TRPM6 in European-Americans: the Atherosclerosis Risk in Communities (ARIC) study. *BMC Genet* 16: 56, 2015. doi:10.1186/s12863-015-0219-7.
16. **Ware EB**, **Smith JA**, **Zhao W**, **Ganesvoort RT**, **Curhan GC**, **Pollak M**, **Mount DB**, **Turner ST**, **Chen G**, **Shah RJ**, **Kardia SLR**, **Lieske JC.** Genome-wide association study of 24-hour urinary excretion of calcium, magnesium, and uric acid. *Mayo Clin Proc Innov Qual Outcomes* 3: 448–460, 2019. doi:10.1016/j.mayocpiqo.2019.08.007.
17. **Svenson KL**, **Gatti DM**, **Valdar W**, **Welsh CE**, **Cheng R**, **Chesler EJ**, **Palmer AA**, **McMillan L**, **Churchill GA.** High-resolution genetic mapping using the Mouse Diversity outbred population. *Genetics* 190: 437–447, 2012. doi:10.1534/genetics.111.132597.
18. **Broman KW**, **Gatti DM**, **Simecek P**, **Furlotte NA**, **Prins P**, **Sen S**[**], **Yandell BS**, **Churchill GA.** R/qtl2: software for mapping quantitative trait loci with high-dimensional data and multiparent populations. *Genetics* 211: 495–502, 2019. doi:10.1534/genetics.118.301595.
19. **Kurstjens S**, **van Diepen JA**, **Overmars-Bos C**, **Alkema W**, **Bindels RJM**, **Ashcroft FM**, **Tack CJJ**, **Hoenderop JGJ**, **de Baaij JHF.** Magnesium deficiency prevents high-fat-diet-induced obesity in mice. *Diabetologia* 61: 2030–2042, 2018. doi:10.1007/s00125-018-4680-5.
20. **van der Hagen EAE**, **Lavrijsen M**, **van Zeeland F**, **Praetorius J**, **Bonny O**, **Bindels RJM**, **Hoenderop JGJ.** Coordinated regulation of TRPV5-mediated $Ca^{2+}$ transport in primary distal convolution cultures. *Pflugers Arch* 466: 2077–2087, 2014. doi:10.1007/s00424-014-1470-x.
21. **Ayuk J**, **Gittoes NJ.** Contemporary view of the clinical relevance of magnesium homeostasis. *Ann Clin Biochem* 51: 179–188, 2014. doi:10.1177/0004563213517628.
22. **Beggs MR**, **Appel I**, **Svenningsen P**, **Skjødt K**, **Alexander RT**, **Dimke H.** Expression of transcellular and paracellular calcium and magnesium transport proteins in renal and intestinal epithelia during lactation. *Am J Physiol Renal Physiol* 313: F629–F640, 2017. doi:10.1152/ajprenal.00680.2016.
23. **van Megen WH**, **Canki E**, **Wagenaar VHA**, **van Waes CRMM**, **Peters DJM**, **Van Asbeck-Van der Wijst J**, **Hoenderop JGJ.** Fluid shear stress stimulates ATP release without regulating purinergic gene expression in the renal inner medullary collecting duct. *FASEB J* 37: e23232, 2023. doi:10.1096/fj.202301434R.
24. **Takemon Y**, **Chick JM**, **Gerdes Gyuricza I**, **Skelly DA**, **Devuyst O**, **Gygi SP**, **Churchill GA**, **Korstanje R.** Proteomic and transcriptomic profiling reveal different aspects of aging in the kidney. *eLife* 10: e62585, 2021. doi:10.7554/eLife.62585.
25. **Yan B**, **Zhang ZZ**, **Huang LY**, **Shen HL**, **Han ZG.** OIT3 deficiency impairs uric acid reabsorption in renal tubule. *FEBS Lett* 586: 760–765, 2012. doi:10.1016/j.febslet.2012.01.038.
26. **Nie M**, **Bal MS**, **Liu J**, **Yang Z**, **Rivera C**, **Wu X-R**, **Hoenderop JGJ**, **Bindels RJM**, **Marciano DK**, **Wolf MTF.** Uromodulin regulates renal magnesium homeostasis through the ion channel transient receptor potential melastatin 6 (TRPM6). *J Biol Chem* 293: 16488–16502, 2018. doi:10.1074/jbc.RA118.003950.
27. **Olinger E**, **Houillier P**, **Devuyst O.** Claudins: a tale of interactions in the thick ascending limb. *Kidney Int* 93: 535–537, 2018. doi:10.1016/j.kint.2017.09.032.
28. **de Baaij JHF.** Magnesium reabsorption in the kidney. *Am J Physiol Renal Physiol* 324: F227–F244, 2023. doi:10.1152/ajprenal.00298.2022.
29. **Moor MB**, **Bonny O.** Ways of calcium reabsorption in the kidney. *Am J Physiol Renal Physiol* 310: F1337–F1350, 2016. doi:10.1152/ajprenal.00273.2015.
30. **Uhlén M**, **Fagerberg L**, **Hallström BM**, **Lindskog C**, **Oksvold P**, **Mardinoglu A et al.** Proteomics. Tissue-based map of the human proteome. *Science* 347: 1260419, 2015. doi:10.1126/science.1260419.
31. **Wu J-X**, **He K-Y**, **Zhang Z-Z**, **Qu Y-L**, **Su X-B**, **Shi Y**, **Wang N**, **Wang L**, **Han Z-G.** LZP is required for hepatic triacylglycerol transportation through maintaining apolipoprotein B stability. *PLoS Genet* 17: e1009357, 2021. doi:10.1371/journal.pgen.1009357.
32. **Xu Z-G**, **Du J-J**, **Zhang X**, **Cheng Z-H**, **Ma Z-Z**, **Xiao H-S**, **Yu L**, **Wang Z-Q**, **Li Y-Y**, **Huo K-K**, **Han Z-G.** A novel liver-specific zona pellucida domain containing protein that is expressed rarely in hepatocellular

carcinoma. *Hepatology* 38: 735–744, 2003. doi:10.1053/jhep.2003.50340.
33. **Shen H-L**, **Xu Z-G**, **Huang L-Y**, **Liu D**, **Lin D-H**, **Cao J-B**, **Zhang X**, **Wang Z-Q**, **Wang W-H**, **Yang P-Y**, **Han Z-G.** Liver-specific ZP domain-containing protein (LZP) as a new partner of Tamm-Horsfall protein harbors on renal tubules. *Mol Cell Biochem* 321: 73–83, 2009. doi:10.1007/s11010-008-9921-3.
34. **Xu Z-G**, **Du J-J**, **Cui S-J**, **Wang Z-Q**, **Huo K-K**, **Li Y-Y**, **Han Z-G.** Identification of LZP gene from *Mus musculus* and *Rattus norvegicus* coding for a novel liver-specific ZP domain-containing secretory protein. *DNA Seq* 15: 81–87, 2004. doi:10.1080/10425170310001652200.
35. **Chen L**, **Chou CL**, **Knepper MA.** A comprehensive map of mRNAs and their isoforms across all 14 renal tubule segments of mouse. *J Am Soc Nephrol* 32: 897–912, 2021. doi:10.1681/ASN.2020101406.
36. **Ransick A**, **Lindström NO**, **Liu J**, **Zhu Q**, **Guo J-J**, **Alvarado GF**, **Kim AD**, **Black HG**, **Kim J**, **McMahon AP.** Single-cell profiling reveals sex, lineage, and regional diversity in the mouse kidney. *Dev Cell* 51: 399–413.e7, 2019. doi:10.1016/j.devcel.2019.10.005.
37. **Wu H**, **Kirita Y**, **Donnelly EL**, **Humphreys BD.** Advantages of single-nucleus over single-cell RNA sequencing of adult kidney: rare cell types and novel cell states revealed in fibrosis. *J Am Soc Nephrol* 30: 23–32, 2019. doi:10.1681/ASN.2018090912.
38. **Li Z-W**, **Ruan B**, **Yang P-J**, **Liu J-J**, **Song P**, **Duan J-L**, **Wang L.** Oit3, a promising hallmark gene for targeting liver sinusoidal endothelial cells. *Signal Transduct Target Ther* 8: 344, 2023. doi:10.1038/s41392-023-01621-2.
39. **Selvaraju S**, **Swathi D**, **Ramya L**, **Lavanya M**, **Archana SS**, **Sivaram M.** Orchestrating the expression levels of sperm mRNAs reveals CCDC174 as an important determinant of semen quality and bull fertility. *Syst Biol Reprod Med* 67: 89–101, 2021. doi:10.1080/19396368.2020.1836286.
40. **De Stefani D**, **Raffaello A**, **Teardo E**, **Szabò I**, **Rizzuto R.** A forty-kilodalton protein of the inner membrane is the mitochondrial calcium uniporter. *Nature* 476: 336–340, 2011. doi:10.1038/nature10230.
41. **Perocchi F**, **Gohil VM**, **Girgis HS**, **Bao XR**, **McCombs JE**, **Palmer AE**, **Mootha VK.** MICU1 encodes a mitochondrial EF hand protein required for $Ca^{2+}$ uptake. *Nature* 467: 291–296, 2010. doi:10.1038/nature09358.
42. **Viering D**, **de Baaij JHF**, **Walsh SB**, **Kleta R**, **Bockenhauer D.** Genetic causes of hypomagnesemia, a clinical overview. *Pediatr Nephrol* 32: 1123–1135, 2017. doi:10.1007/s00467-016-3416-3.
43. **Viering D**, **Schlingmann KP**, **Hureaux M**, **Nijenhuis T**, **Mallett A**, **Chan MMY**, **van Beek A**, **van Eerde AM**, **Coulibaly JM**, **Vallet M**, **Decramer S**, **Pelletier S**, **Klaus G**, **Kömhoff M**, **Beetz R**, **Patel C**, **Shenoy M**, **Steenbergen EJ**, **Anderson G**, **Bongers EMHF**, **Bergmann C**, **Panneman D**, **Rodenburg RJ**, **Kleta R**, **Houillier P**, **Konrad M**, **Vargas-Poussou R**, **Knoers NVAM**, **Bockenhauer D**, **de Baaij JHF**; **Genomics England Research Consortium**. Gitelman-like syndrome caused by pathogenic variants in mtDNA. *J Am Soc Nephrol* 33: 305–325, 2022. doi:10.1681/ASN.2021050596.
44. **Kaissling B**, **Le Hir M.** Distal tubular segments of the rabbit kidney after adaptation to altered Na- and K-intake. I. Structural changes. *Cell Tissue Res* 224: 469–492, 1982. doi:10.1007/BF00213746.
45. **McCormick JA**, **Ellison DH.** Distal convoluted tubule. *Compr Physiol* 5: 45–98, 2015. doi:10.1002/cphy.c140002.
46. **Nassar LR**, **Barber GP**, **Benet-Pagès A**, **Casper J**, **Clawson H**, **Diekhans M**, **Fischer C**, **Gonzalez JN**, **Hinrichs AS**, **Lee BT**, **Lee CM**, **Muthuraman P**, **Nguy B**, **Pereira T**, **Nejad P**, **Perez G**, **Raney BJ**, **Schmelter D**, **Speir ML**, **Wick BD**, **Zweig AS**, **Haussler D**, **Kuhn RM**, **Haeussler M**, **Kent WJ.** The UCSC Genome Browser database: 2023 update. *Nucleic Acids Res* 51: D1188–D1195, 2023. doi:10.1093/nar/gkac1072.
47. **de Baaij JHF**, **Arjona FJ**, **van den Brand M**, **Lavrijsen M**, **Lameris ALL**, **Bindels RJM**, **Hoenderop JGJ.** Identification of SLC41A3 as a novel player in magnesium homeostasis. *Sci Rep* 6: 28565, 2016. doi:10.1038/srep28565.
48. **Franken GAC**, **Seker M**, **Bos C**, **Siemons LAH**, **van der Eerden BCJ**, **Christ A**, **Hoenderop JGJ**, **Bindels RJM**, **Müller D**, **Breiderhoff T**, **de Baaij JHF.** Cyclin M2 (CNNM2) knockout mice show mild hypomagnesaemia and developmental defects. *Sci Rep* 11: 8217, 2021. doi:10.1038/s41598-021-87548-6.
49. **Groenestege WMT**, **Hoenderop JG**, **van den Heuvel L**, **Knoers N**, **Bindels RJ.** The epithelial $Mg^{2+}$ channel transient receptor potential melastatin 6 is regulated by dietary $Mg^{2+}$ content and estrogens. *J Am Soc Nephrol* 17: 1035–1043, 2006. doi:10.1681/ASN.2005070700.
50. **van Angelen AA**, **San-Cristobal P**, **Pulskens WP**, **Hoenderop JG**, **Bindels RJ.** The impact of dietary magnesium restriction on magnesiotropic and calciotropic genes. *Nephrol Dial Transplant* 28: 2983–2993, 2013. doi:10.1093/ndt/gft358.
51. **Corre T**, **Olinger E**, **Harris SE**, **Traglia M**, **Ulivi S**, **Lenarduzzi S**, **Belge H**, **Youhanna S**, **Tokonami N**, **Bonny O**, **Houillier P**, **Polasek O**, **Deary IJ**, **Starr JM**, **Toniolo D**, **Gasparini P**, **Vollenweider P**, **Hayward C**, **Bochud M**, **Devuyst O.** Common variants in CLDN14 are associated with differential excretion of magnesium over calcium in urine. *Pflugers Arch* 469: 91–103, 2017. doi:10.1007/s00424-016-1913-7.
52. **Ferreira PG**, **van Megen WH**, **Tan R**, **Lee CHL**, **Svenningsen P**, **Alexander RT**, **Dimke H.** Renal claudin-14 expression is not required for regulating $Mg^{2+}$ balance in mice. *Am J Physiol Renal Physiol* 320: F897–F907, 2021. doi:10.1152/ajprenal.00590.2020.
53. **Anast CS**, **Mohs JM**, **Kaplan SL**, **Burns TW.** Evidence for parathyroid failure in magnesium deficiency. *Science* 177: 606–608, 1972. doi:10.1126/science.177.4049.606.
54. **Quitterer U**, **Hoffmann M**, **Freichel M**, **Lohse MJ.** Paradoxical block of parathormone secretion is mediated by increased activity of Gα subunits. *J Biol Chem* 276: 6763–6769, 2001. doi:10.1074/jbc.M007727200.
55. **Suh SM**, **Tashjian AH Jr**, **Matsuo N**, **Parkinson DK**, **Fraser D.** Pathogenesis of hypocalcemia in primary hypomagnesemia: normal end-organ responsiveness to parathyroid hormone, impaired parathyroid gland function. *J Clin Invest* 52: 153–160, 1973. doi:10.1172/JCI107159.
56. **Vetter T**, **Lohse MJ.** Magnesium and the parathyroid. *Curr Opin Nephrol Hypertens* 11: 403–410, 2002. doi:10.1097/00041552-200207000-00006.
57. **Alexander RT**, **Dimke H.** Effects of parathyroid hormone on renal tubular calcium and phosphate handling. *Acta Physiol (Oxf)* 238: e13959, 2023. doi:10.1111/apha.13959.
58. **Hoenderop JG**, **van der Kemp AW**, **Hartog A**, **van de Graaf SF**, **van Os CH**, **Willems PH**, **Bindels RJ.** Molecular identification of the apical $Ca^{2+}$ channel in 1,25-dihydroxyvitamin $D_3$-responsive epithelia. *J Biol Chem* 274: 8375–8378, 1999. doi:10.1074/jbc.274.13.8375.
59. **Reilly RF**, **Shugrue CA**, **Lattanzi D**, **Biemesderfer D.** Immunolocalization of the $Na^+/Ca^{2+}$ exchanger in rabbit kidney. *Am J Physiol Renal Physiol* 265: F327–F332, 1993. doi:10.1152/ajprenal.1993.265.2.F327.
60. **Ferdaus MZ**, **Mukherjee A**, **Nelson JW**, **Blatt PJ**, **Miller LN**, **Terker AS**, **Staub O**, **Lin D-H**, **McCormick JA.** $Mg^{2+}$ restriction downregulates NCC through NEDD4-2 and prevents its activation by hypokalemia. *Am J Physiol Renal Physiol* 317: F825–F838, 2019. doi:10.1152/ajprenal.00216.2019.
61. **Tahaei E**, **Coleman R**, **Saritas T**, **Ellison DH**, **Welling PA.** Distal convoluted tubule sexual dimorphism revealed by advanced 3D imaging. *Am J Physiol Renal Physiol* 319: F754–F764, 2020. doi:10.1152/ajprenal.00441.2020.
62. **Yang L**, **Frindt G**, **Palmer LG.** Magnesium modulates ROMK channel-mediated potassium secretion. *J Am Soc Nephrol* 21: 2109–2116, 2010. doi:10.1681/ASN.2010060617.
63. **Huang CL**, **Kuo E.** Mechanism of hypokalemia in magnesium deficiency. *J Am Soc Nephrol* 18: 2649–2652, 2007. doi:10.1681/ASN.2007070792.
64. **Hess MW**, **de Baaij JHF**, **Broekman MMTJ**, **Bisseling TM**, **Haarhuis BJT**, **Tan ACITL**, **Te Morsche RHM**, **Hoenderop JGJ**, **Bindels RJM**, **Drenth JPH.** Common single nucleotide polymorphisms in transient receptor potential melastatin type 6 increase the risk for proton pump inhibitor-induced hypomagnesemia: a case-control study. *Pharmacogenet Genomics* 27: 83–88, 2017. doi:10.1097/FPC.0000000000000259.
65. **Kieboom BCT**, **Ligthart S**, **Dehghan A**, **Kurstjens S**, **de Baaij JHF**, **Franco OH**, **Hofman A**, **Zietse R**, **Stricker BH**, **Hoorn EJ.** Serum magnesium and the risk of prediabetes: a population-based cohort study. *Diabetologia* 60: 843–853, 2017. doi:10.1007/s00125-017-4224-4.
66. **Funato Y**, **Yamazaki D**, **Okuzaki D**, **Yamamoto N**, **Miki H.** Importance of the renal ion channel TRPM6 in the circadian secretion of renin to raise blood pressure. *Nat Commun* 12: 3683, 2021. doi:10.1038/s41467-021-24063-2.
67. **Nair AV**, **Hocher B**, **Verkaart S**, **van Zeeland F**, **Pfab T**, **Slowinski T**, **Chen Y-P**, **Schlingmann KP**, **Schaller A**, **Gallati S**, **Bindels RJ**,

**Konrad M**, **Hoenderop JG.** Loss of insulin-induced activation of TRPM6 magnesium channels results in impaired glucose tolerance during pregnancy. *Proc Natl Acad Sci USA* 109: 11324–11329, 2012. doi:10.1073/pnas.1113811109.

68. **Song Y**, **Hsu YH**, **Niu T**, **Manson JE**, **Buring JE**, **Liu S.** Common genetic variants of the ion channel transient receptor potential membrane melastatin 6 and 7 (TRPM6 and TRPM7), magnesium intake, and risk of type 2 diabetes in women. *BMC Med Genet* 10: 4, 2009. doi:10.1186/1471-2350-10-4.
69. **Chang AM**, **Halter JB.** Aging and insulin secretion. *Am J Physiol Endocrinol Physiol* 284: E7–E12, 2003. doi:10.1152/ajpendo.00366.2002.
70. **Cao G**, **van der Wijst J**, **van der Kemp A**, **van Zeeland F**, **Bindels RJ**, **Hoenderop JG.** Regulation of the epithelial $Mg^{2+}$ channel TRPM6 by estrogen and the associated repressor protein of estrogen receptor activity (REA). *J Biol Chem* 284: 14788–14795, 2009. doi:10.1074/jbc.M808752200.
71. **Habermehl TL**, **Underwood KB**, **Welch KD**, **Gawrys SP**, **Parkinson KC**, **Schneider A**, **Masternak MM**, **Mason JB.** Aging-associated changes in motor function are ovarian somatic tissue-dependent, but germ cell and estradiol independent in post-reproductive female mice exposed to young ovarian tissue. *Geroscience* 44: 2157–2169, 2022. doi:10.1007/s11357-022-00549-9.
72. **Chubanov V**, **Ferioli S**, **Wisnowsky A**, **Simmons DG**, **Leitzinger C**, **Einer C**, **Jonas W**, **Shymkiv Y**, **Bartsch H**, **Braun A**, **Akdogan B**, **Mittermeier L**, **Sytik L**, **Torben F**, **Jurinovic V**, **van der Vorst EP**, **Weber C**, **Yildirim ÖA**, **Sotlar K**, **Schürmann A**, **Zierler S**, **Zischka H**, **Ryazanov AG**, **Gudermann T.** Epithelial magnesium transport by TRPM6 is essential for prenatal development and adult survival. *eLife* 5: e20914, 2016. doi:10.7554/eLife.20914.
73. **Börsch A**, **Ham DJ**, **Mittal N**, **Tintignac LA**, **Migliavacca E**, **Feige JN**, **Rüegg MA**, **Zavolan M.** Molecular and phenotypic analysis of rodent models reveals conserved and species-specific modulators of human sarcopenia. *Commun Biol* 4: 194, 2021. doi:10.1038/s42003-021-01723-z.
74. **Eisner C**, **Faulhaber-Walter R**, **Wang Y**, **Leelahavanichkul A**, **Yuen PST**, **Mizel D**, **Star RA**, **Briggs JP**, **Levine M**, **Schnermann J.** Major contribution of tubular secretion to creatinine clearance in mice. *Kidney Int* 77: 519–526, 2010. doi:10.1038/ki.2009.501.